Note: This copy is for your personal, non-commercial use only. To order presentation-ready copies for distribution to your colleagues or clients, use the *Radiology* Reprints form at the end of this article.

Radiology

Carotid Artery Brain Aneurysm Model: In Vivo Molecular Enzyme-specific MR Imaging of Active Inflammation in a Pilot Study[1]

Michael J. DeLeo III, BA
Matthew J. Gounis, PhD
Bo Hong, MD[2]
John C. Ford, PhD
Ajay K. Wakhloo, MD, PhD
Alexei A. Bogdanov, Jr, PhD

Purpose: To demonstrate the feasibility of using a myeloperoxidase (MPO)-specific paramagnetic magnetic resonance (MR) contrast agent to identify active inflammation in an animal model of common carotid artery (CCA) aneurysm.

Materials and Methods: All animal experiments were approved by the institutional animal care and use committee. Elastase-induced saccular aneurysms were created at the root of the right CCA in 16 New Zealand white rabbits. Intramural and perivascular injection of *Escherichia coli* lipopolysaccharide (LPS) was performed with an endovascular approach to induce aneurysm inflammation. After intraarterial injection of an MPO-specific (di-5-hydroxytryptamide of gadopentetate dimeglumine, 0.1 mmol per kilogram of bodyweight) or a non–MPO-specific (di-tyrosine of gadopentetate dimeglumine, 0.1 mmol/kg) contrast agent, animals underwent 3-T MR imaging. Intramural presence of MPO in aneurysms in which LPS had been injected was confirmed at immunohistologic analysis. Active MPO activity was verified by measuring the spectrophotometric oxidation of guaiacol.

Results: Endovascular injection of LPS resulted in inflammatory cell infiltration into the aneurysm wall, and there was a difference in active MPO expression between aneurysms in which LPS had been injected and control aneurysms (20.3 ng of MPO per milligram of tissue vs 0.12 ng of MPO per milligram of tissue, respectively; $P < .002$). MR imaging with di-5-hydroxytryptamide of gadopentetate dimeglumine revealed a difference in enhancement ratio between inflamed aneurysms in which LPS had been injected and control aneurysms (1.55 ± 0.05 vs 1.16 ± 0.10, respectively; $P < .02$). In inflamed aneurysms, di-5-hydroxytryptamide of gadopentetate dimeglumine exhibited delayed washout kinetics compared with the kinetics of di-tyrosine of gadopentetate dimeglumine. This finding enabled the verification of MPO specificity.

Conclusion: The findings of this pilot study established the feasibility of an animal model of saccular aneurysm inflammation that can be seen with clinical-field-strength MR imaging and use of the enzyme-sensitive MR contrast agent di-5-hydroxytryptamide of gadopentetate dimeglumine, which is a paramagnetic MPO substrate that specifically enhances MR signal.

© RSNA, 2009

[1] From the Department of Radiology (M.J.D., M.J.G., B.H., J.C.F., A.K.W., A.A.B.) and New England Center for Stroke Research (M.J.G., B.H., A.K.W.), University of Massachusetts Medical School, 55 Lake Ave North, Worcester, MA 01655. From the 2008 RSNA Annual Meeting. Received August 11; revision requested October 2; revision received December 25; accepted February 5, 2009; final version accepted February 16. **Address correspondence to** A.K.W. (e-mail: *WakhlooA@ummhc.org*).
[2] **Current address:** Department of Neurosurgery, Changhai Hospital, 2nd Military Medical University, Shanghai, China.

© RSNA, 2009

In the United States, an estimated 1 million to 12 million people (1%–6%) harbor unruptured intracranial aneurysms (IAs) (1). Of the 27 000 people who experience aneurysmal subarachnoid hemorrhage annually, almost half die within 30 days after the event (2,3). Management of an unruptured IA is controversial. Primarily on the basis of natural history data compiled by the International Study on Unruptured Intracranial Aneurysms investigators (4,5), when making a clinical decision, physicians usually take into account the patient's age and attitude, the aneurysm size and location, and the skills of local neurosurgeons and neuroendovascular interventionalists (6). Treatment options (microsurgical clip placement and endovascular coil embolization) carry associated risks; therefore, it is imprudent to treat unruptured IA in all patients. Since most asymptomatic IA ruptures occur without warning, there is a pressing need to develop techniques with which to identify unstable aneurysms, especially since the use of advanced imaging modalities increases the number of unruptured IAs detected in the general population (7).

IA pathogenesis is a complex multifactorial process that includes hemodynamic sheer stress (8), certain genetic modifiers (9), and inflammatory changes (10–13) that may contribute to instability of the aneurysm wall. Extracellular matrix degradation secondary to macrophage infiltration is thought to play a large role (12,13). Ruptured IAs are associated with more acute intramural inflammation, as characterized by the infiltration of neutrophils and macrophages (11,14). These two inflammatory cell types express myeloperoxidase (MPO), which is a heme-containing oxidoreductase enzyme that functions primarily as a secretable microbicidal enzyme (15). MPO released into the extracellular space by activated inflammatory cells can induce the intramural formation of highly reactive free radicals (16) and contribute to extracellular matrix degradation by either activating matrix metalloproteinases (17) or inactivating matrix metalloproteinase inhibitors (18). As a result, MPO has been implicated in several disease processes, such as lung and renal injury, carcinogenesis, and atherosclerosis (19).

In consideration of the correlation between inflammation and IA rupture and the lack of diagnostic imaging methods that can be used to identify IA inflammation, we hypothesize that MPO-specific magnetic resonance (MR) signal enhancement could represent a biomarker of IA instability. The purpose of this pilot study was to demonstrate the feasibility of using an MPO-specific paramagnetic MR contrast agent to identify active inflammation in an animal model of common carotid artery (CCA) aneurysm.

Advances in Knowledge

- Experimental common carotid artery aneurysm inflammation can be induced by endovascular delivery of proinflammatory agents.
- Molecular enzyme-specific MR imaging of active inflammation is feasible in an animal model of aneurysm inflammation.

Materials and Methods

Aneurysm Creation and Inflammation Induction

All animal experiments were performed in accordance with a protocol approved by our institutional animal care and use committee. Anesthesia was induced in 16 New Zealand white rabbits with intramuscular injection of ketamine (35 mg per kilogram of body weight), xylazine (5 mg/kg), and glycopyrrolate (0.01 mg/kg) and maintained with 1%–2% isoflurane at endotracheal intubation. All rabbits received 12–15 U of elastase (Sigma-Aldrich, St Louis, Mo) to create an elastase–induced saccular aneurysm at the root of the right CCA, as described previously (20,21).

After a 21-day maturation and stabilization period, aneurysm morphology was assessed with three-dimensional reconstructive x-ray angiography (Allura FD20; Philips Healthcare, Best, the Netherlands). Two authors (M.J.G., B.H.; both of whom had 10 years of experience) performed the angiographic procedures. They used an endovascular approach to advance a modified delivery tube through the aneurysm wall (Fig 1) and intramurally and perivascularly inject 200 μL of 5 μg/mL *Escherichia coli* lipopolysaccharide (LPS) (Sigma-Aldrich) in saline to induce inflammation (22). Control animals did not undergo any additional surgical or endovascular procedures after initial aneurysm creation. Two authors (M.J.D., A.A.B.) prepared gold (approximately 35 nm) nanoparticle colloids with gold chloride (115 μg/mL, Sigma-Aldrich) colloidal nucleation in the presence of citrate, as described previously (23). The colloid was concentrated by centrifugation at 80 000*g* and injected into a subset of two animals with either LPS or saline to enable visualization of the injection site with fluoroscopy.

In one animal, there was incomplete balloon occlusion of the proximal right CCA during aneurysm creation, which resulted in elastase leakage into the circulation. The animal was found dead 5 days after the procedure. Necropsy revealed gross hemorrhage of the lungs. This animal was not available for data collection. Another animal was excluded from analysis after death secondary to anesthesia overdose during postcontrast MR imaging. In the final MR image analysis, a total of 10 animals were included in the control

Published online before print
10.1148/radiol.2523081426

Radiology 2009; 252:696–703

Abbreviations:
CCA = common carotid artery
IA = intracranial aneurysm
LPS = lipopolysaccharide
MPO = myeloperoxidase

Author contributions:
Guarantors of integrity of entire study, M.J.D., A.A.B.; study concepts/study design or data acquisition or data analysis/interpretation, all authors; manuscript drafting or manuscript revision for important intellectual content, all authors; manuscript final version approval, all authors; literature research, M.J.D., M.J.G., A.K.W., A.A.B.; experimental studies, all authors; statistical analysis, M.J.D., M.J.G., J.C.F.; and manuscript editing, M.J.D., M.J.G., J.C.F., A.K.W., A.A.B.

Funding:
This research was supported by the National Institutes of Health (grants NINDS R21NS061132 and NIBIB R21 EB007767).

Authors stated no financial relationship to disclose.

See also Science to Practice in this issue.

($n = 5$) and LPS ($n = 5$) groups. Four additional animals that had aneurysms with LPS-induced inflammation underwent sequential MR imaging at multiple time points with MPO-specific ($n = 2$) and non–MPO-specific ($n = 2$) contrast agents, as will be described in the next section.

MPO-specific and Non–MPO-specific Contrast Agents

An author (A.A.B., 18 years of experience) performed synthesis of MPO-specific (di-5-hydroxytryptamide of gadopentetate dimeglumine) and non–MPO-specific (di-tyrosine of gadopentetate dimeglumine) MR contrast agents, as described previously (24,25), with slight modifications. Briefly, for the synthesis of di-5-hydroxytryptamide of gadopentetate dimeglumine, 5.6 mmol of diethylenetriaminepentaacetic acid bis anhydride (Sigma-Aldrich) was reacted with 2.2 mol/L equivalents of serotonin (5-hydroxytryptamine) hydrochloride (Tokyo Chemical Industry America, Portland, Ore) in dimethylformamide in the presence of a 2.5 mol/L equivalent of triethylamine under argon at 70°C with refluxing for 6 hours. For synthesis of the non–MPO-specific agent, tyramine was substituted for serotonin, and synthesis was performed, as will be described later. After cooling, 5% $NaHCO_3$ in water was added, the mixture was stirred, and solvents were removed with a vacuum. To obtain gadolinium salt, di-5-hydroxytryptamide-diethylenetriaminepentaacetic acid was dissolved in a solution of 1.2 mol/L excess of gadolinium chloride in 1% sodium citrate adjusted with acetic acid to have a pH of 6.5. After the solutions had been stored for 48 hours at room temperature, the solvents were removed with a vacuum and underwent precipitation twice with boiling methanol and water (9:1 vol/vol) by using acetone. The dried product was purified on carbon-18 high-performance liquid chromotography column, lyophilized, and tested by measuring longitudinal relaxivity before and after adding horseradish peroxidase/H_2O_2, as described previously (24). A 2.3–2.4-fold increase in relaxivity was considered acceptable for further use in animal experiments.

MR Imaging

Forty-eight hours after LPS injection, the animals were anesthetized as described previously and imaged with a 3-T whole-body MR unit (Achieva; Philips Healthcare). Each rabbit was carefully positioned in the center of an eight-element receive-only knee coil (SENSE; Philips Healthcare). Radiofrequency transmission was performed with the built-in quadrature body coil. Precontrast time-of-flight MR angiography was performed 48 hours after LPS injection to assess aneurysm patency, primarily to rule out thrombosis of the aneurysm. The first pulse sequence used for analysis was a 3-minute 38-second T1-weighted three-dimensional fast field-echo sequence (repetition time msec/echo time msec, 17.9/2.3; 25° flip angle; 434.5 Hz/pixel bandwidth; 120-mm field of view; 192 × 192 matrix; 0.63 × 0.63 × 2-mm resolution; four signals acquired). A 2-minute 32-second three-dimensional time-of-flight MR angiographic sequence was then performed (23/3.5, 20° flip angle, 217.2 Hz/pixel bandwidth, 80-mm field of view, 448 × 115 matrix, 0.33 × 0.66 × 1.2-mm resolution, two signals acquired). Animals were then injected with a sterile solution of 0.1 mmol/kg of di-5-hydroxytryptamide of gadopentetate dimeglumine or di-tyrosine of gadopentetate dimeglumine in 15 mL of 5% meglumine with a pH of 7. Imaging was performed again 3 hours later with the same imaging parameters. Time course experiments were performed up to 330 minutes after contrast agent injection with the same imaging parameters described previously after administration of either di-5-hydroxytryptamide of gadopentetate dimeglumine or di-tyrosine of gadopentetate dimeglumine in ani-

Figure 1

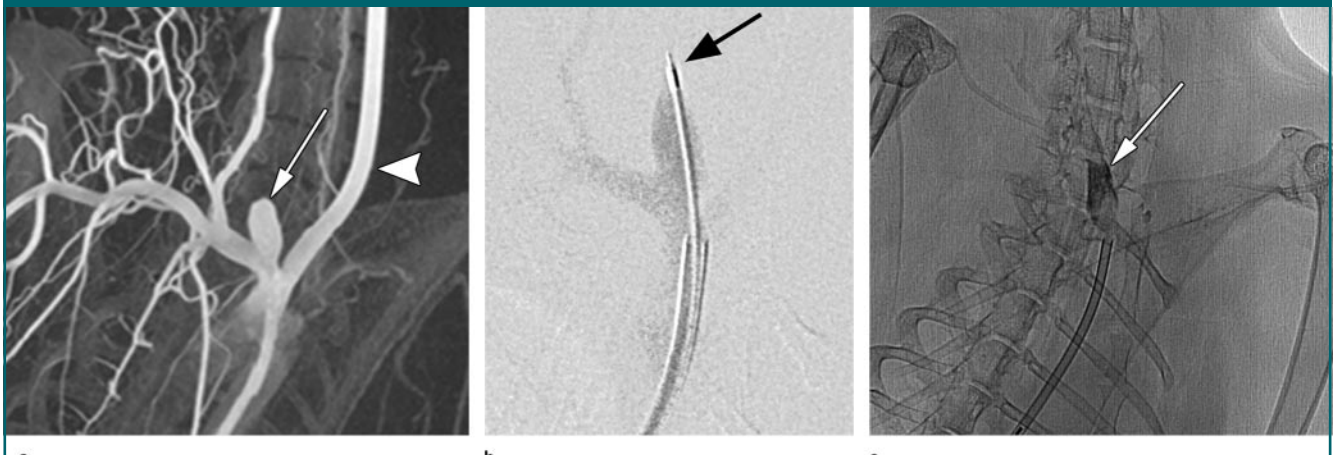

Figure 1: Oblique **(a)** reconstructed three-dimensional x-ray angiogram, **(b)** digital subtraction angiogram, and **(c)** radiograph. In **a**, an elastase-induced aneurysm (arrow) and the left CCA (arrowhead) are visible. In **b**, positioning of the LPS delivery tube (arrow) though the dome of the aneurysm is shown, and in **c**, gold nanoparticles, which enabled us to confirm the perivascular injection of LPS (arrow) are visible.

mals with aneurysms into which LPS had been injected.

Immunohistochemistry

Immediately after MR imaging, animals were killed with intravenous injection of 100 mg/kg of pentobarbital. Thereafter, the aneurysm and left CCA were resected and rinsed in saline. The dome of the aneurysm was divided longitudinally: Half of the specimen was transferred to 4% paraformaldehyde, and the other half was snap frozen in liquid nitrogen for subsequent measurement of MPO activity. The left CCA specimen was treated in a similar fashion. After overnight fixation, the tissues were embedded in paraffin and cut into 5-μm-thick slices. Heat-induced epitope retrieval was performed (M.J.D.) for 20 minutes at 95°C in a tris-ethylenediaminetetraacetic acid (10 mg/L and 1 mg/L, respectively) solution with a pH of 9. Slides were blocked for 1 hour in 5% horse serum and then incubated with either 1.5 μg/mL digoxigenin-labeled mouse antihuman MPO antibody (Roche, Indianapolis, Ind) or 5 μg/mL mouse antihuman MAC387 antibody (Abcam, Cambridge, Mass) diluted in 5% horse serum for 1 hour at room temperature. Both antibodies are known to cross-react with rabbit antigens. At washing, slides were incubated with 0.4 μU/mL antidigoxigenin alkaline phosphatase (Roche) diluted in 5% horse serum for 30 minutes. Color was developed with nitro blue tetrazolium chloride/5-bromo-4-chloro-3-inlolyl phosphate (Vector Labs, Burlingame, Calif) chromagen incubation for 30 minutes at RT. Slides were lightly counterstained with either hematoxylin-eosin or nuclear fast red (Vector Labs, Burlingame, Calif) then dehydrated, cleared in xylene, and mounted in permanent mounting media (Permount; Fisher Scientific, Pittsburgh, Pa). Negative controls were performed in the absence of a primary antibody.

MPO Activity Assay

MPO activity was measured (M.J.D.) in aneurysms and the left CCA of control animals and those that received LPS. Tissues frozen in liquid nitrogen as described previously were stored at −80°C until analysis. Briefly, tissues were weighed, thawed, and homogenized in 10 volumes of 0.5% hexadecyltrimethylammonium buffer solution. Homogenates were centrifuged at 13*g* for 20 minutes, and 50-μL supernatant was added to 1 mL of 50 mmol/L potassium phosphate buffer containing 100 mmol/L guaiacol and 0.0017% hydrogen peroxide. Initial rates of change in absorbance at 470 nm were measured against a standard curve by using purified human MPO (Meridian Life Sciences, Saco, Me). Results were expressed in nanograms of MPO per milligram of tissue after determination of the amount of total protein in each sample.

MR Image and Statistical Analyses

Two authors (M.J.G., M.J.D.) performed blinded analysis of the MR images with ImageJ software (National Institutes of Health, Bethesda, Md). For each image, regions of interest were placed over the aneurysm, left CCA, and pectoralis secundus muscle in the same planes as both vascular structures. Mean signal intensity of the aneurysm (SI_A), left CCA (SI_{CCA}), and pectoralis secundus muscle (SI_M) were measured for each region. From images acquired before and after contrast agent administration, signal intensities were measured and normalized by using SI_M as the reference standard. Enhancement ratio of the aneurysm (ER_A) was calculated with the following equation: $ER_A = (SI_{Apost}/SI_{Mpost})/SI_{Apre}/SI_{Mpre})$, where the designators "pre" and "post" indicate before and after contrast agent administration, respectively. For comparison, enhancement ratio of the left CCA (ER_{CCA}) was calculated with the following equation: $ER_{CCA} = (SI_{CCApost}/SI_{Mpost})/SI_{CCApre}/SI_{Mpre})$. Statistical analysis of MR images and MPO activity was performed with the Mann-Whitney test (GraphPad InStat software, version 3.06; GraphPad Software, San Diego, Calif). $P < .05$ indicated a significant difference.

Results

LPS Injection and Increased Intramural MPO in Aneurysms

Hematoxylin-eosin staining of elastase-induced aneurysms revealed the morphology of control aneurysms and LPS-injected aneurysms (Fig 2). Control aneurysms were negative for MPO while LPS-injected aneurysms were strongly positive for MPO. MPO expression was primarily intramural, and in most histologic slices, a progression of cellular infiltration from the luminal side to the adventitial side of the aneurysm wall could be appreciated. At immunohistochemical staining with the MAC387 antibody, we verified that there were no inflammatory cell infiltrates in control aneurysms, while LPS-injected aneurysms had strong MAC387-positive cellular infiltration (neutrophils and macrophages) into aneurysm walls. Analysis performed in the absence of a primary antibody did not reveal any appreciable nonspecific staining. There was a difference in MPO activity as measured with MPO guaiacol oxidation between LPS-injected aneurysms and control aneurysms (20.3 ng of MPO per milligram of tissue vs 0.12 ng of MPO per milligram of tissue, respectively; $P < .002$). There was also a difference in MPO activity between the LPS-injected aneurysms and left CCA vessels in both control animals and LPS-injected animals (0.38 ng of MPO per milligram of tissue vs 0.63 ng of MPO per milligram of tissue, respectively) (Fig 2).

Sensitivity and Specificity for MPO in Inflamed Aneurysms

The kinetics of enhancement of the aneurysm and left CCA with both di-5-hydroxytryptamide of gadopentetate dimeglumine and di-tyrosine of gadopentetate dimeglumine are shown in Figure 3. The enhancement ratio of the inflamed aneurysm in the animal that received di-5-hydroxytryptamide of gadopentetate dimeglumine remained elevated throughout the entire time course of this study when compared with that of the left CCA in the same animal. Both the inflamed aneurysm and the left CCA in the animal that received di-tyrosine of gadopentetate dimeglumine had similar enhancement ratios measured at each point of the time course. These data provide the rationale for choosing the time point of 3 hours after contrast agent administration for final enhancement ratio analysis.

MPO-specific Contrast Agent Targets MPO in Inflamed Aneurysms

Postcontrast T1-weighted fast field-echo MR images demonstrated a difference be-

tween the enhancement ratio of the aneurysm in animals injected with LPS and that in control animals (Fig 4) (1.55 ± 0.05 vs 1.16 ± 0.10, respectively; $P < .02$). There was no significant difference between the enhancement ratio of the CCA in animals injected with LPS and that in control animals (1.66 ± 0.47 vs 1.63 ± 0.43, respectively). In the control group, there was no difference between enhancement ratio of the aneurysm and enhancement ratio of the CCA; however, in the animals injected with LPS, there was a significant difference between enhancement ratio of the aneurysm and enhancement ratio of the CCA ($P < .02$) (Fig 4).

Discussion

In this article, we have described an animal model of saccular aneurysm inflammation that can be depicted with clinical-field-strength MR imaging and use of the enzyme-sensitive MR contrast agent di-5-hydroxytryptamide of gadopentetate dimeglumine, which is a paramagnetic myeloperoxidase substrate that enhances MR signal in an enzyme-specific manner (25). The MR signal enhancement effect is based on increased longitudinal relaxivity of the products of MPO-mediated substrate oxidation (25). As described before (24), the use of low-molecular-weight gadopentetate dimeglumine–based MR contrast agents is relevant because they have been approved by the Food and Drug Administration, and their bismonomethylamide derivatives are nontoxic. Furthermore, we administered a contrast agent dose of 0.1 mmol/kg, which was consistent with clinical gadopentetate dimeglumine doses in humans (26). Therefore, MR imaging of inflammation in the

Figure 2

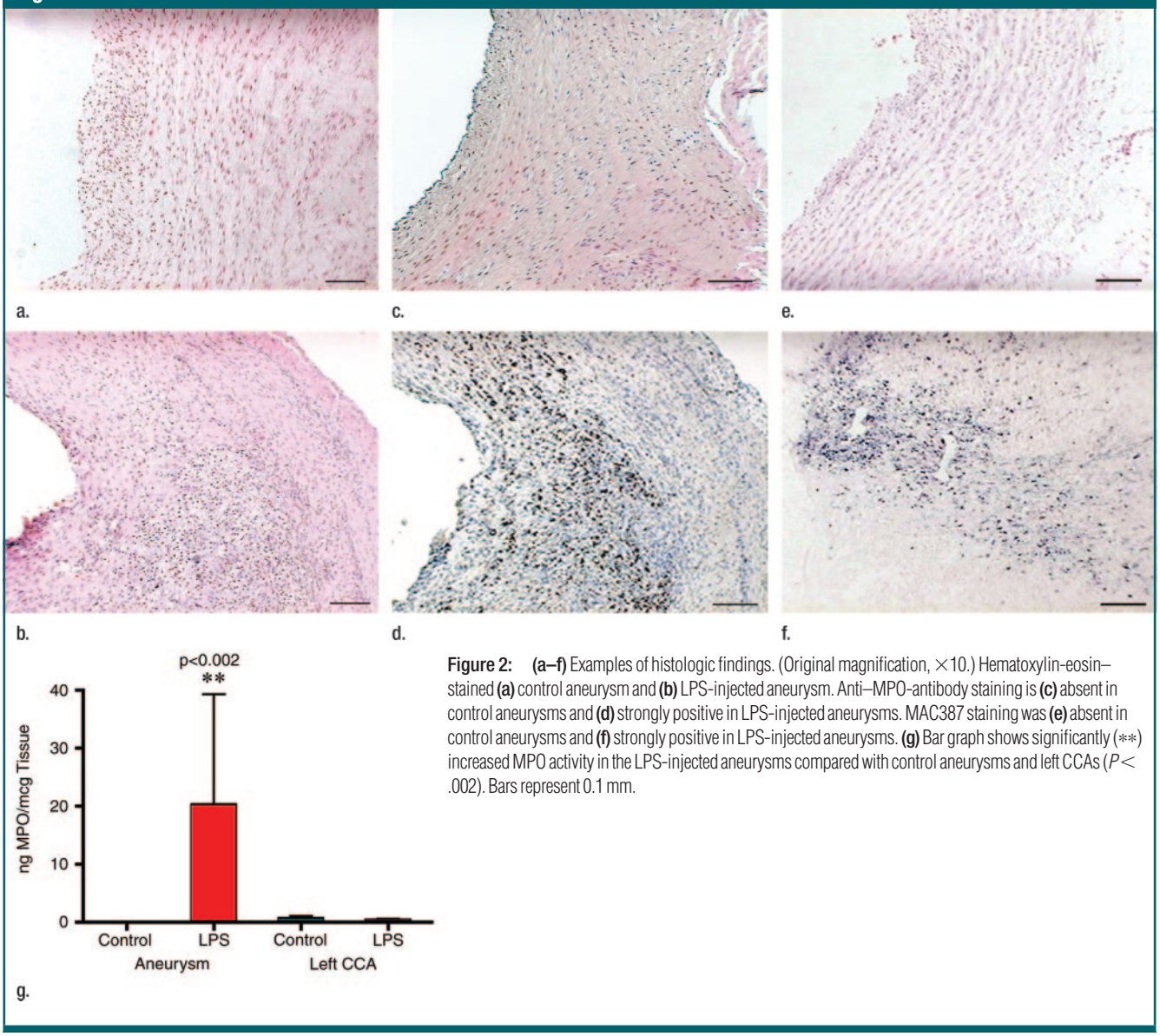

Figure 2: **(a–f)** Examples of histologic findings. (Original magnification, ×10.) Hematoxylin-eosin–stained **(a)** control aneurysm and **(b)** LPS-injected aneurysm. Anti–MPO-antibody staining is **(c)** absent in control aneurysms and **(d)** strongly positive in LPS-injected aneurysms. MAC387 staining was **(e)** absent in control aneurysms and **(f)** strongly positive in LPS-injected aneurysms. **(g)** Bar graph shows significantly (**) increased MPO activity in the LPS-injected aneurysms compared with control aneurysms and left CCAs ($P <$ .002). Bars represent 0.1 mm.

aneurysm wall with di-5-hydroxytryptamide of gadopentetate dimeglumine has the potential to translate into clinical use.

MR imaging is an attractive modality because of its nonionizing properties and high spatial resolution with excellent soft-tissue contrast. The development of contrast agents for use in molecular imaging has the potential to increase the specificity of MR imaging techniques. Relatively recently, enzyme-mediated aggregation of gadolinium-serotonin chelates has been described both in vitro (27) and in vivo (28,29). The mechanism of action of di-5-hydroxytryptamide of gadopentetate dimeglumine involves enzyme-mediated structural changes that lead to accumulation (oligomerization) and retention (covalent bond formation with amino acids) at the site of MPO activity (eg, as a result of covalent bond formation with tyrosine residues of local proteins) (25). Previous study results have shown that MPO is highly selective for di-5-hydroxytryptamide of gadopentetate dimeglumine, leading to an increase in relaxation rate (25). As mentioned previously, we measured longitudinal relaxivity of di-5-hydroxytryptamide of gado-

Figure 3

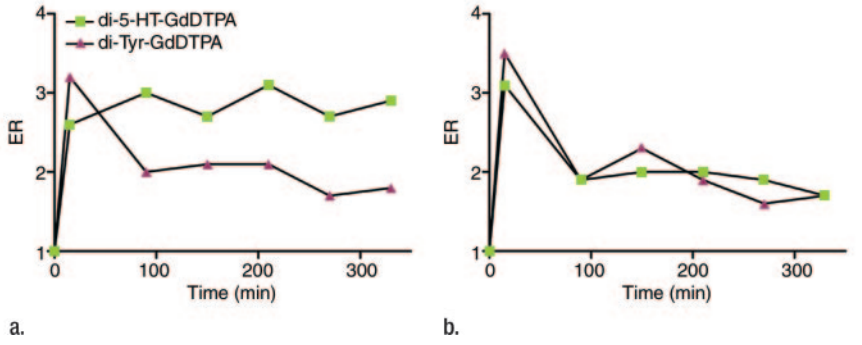

Figure 3: Graphs show kinetics of enhancement of **(a)** a representative LPS-injected aneurysm and **(b)** the left CCA. The enhancement ratio *(ER)* of di-5-hydroxytryptamide of gadopentetate dimeglumine *(di-5-HT-GdDTPA)* is compared with that of di-tyrosine of gadopentetate dimeglumine *(di-Tyr-GdDTPA).*

Figure 4

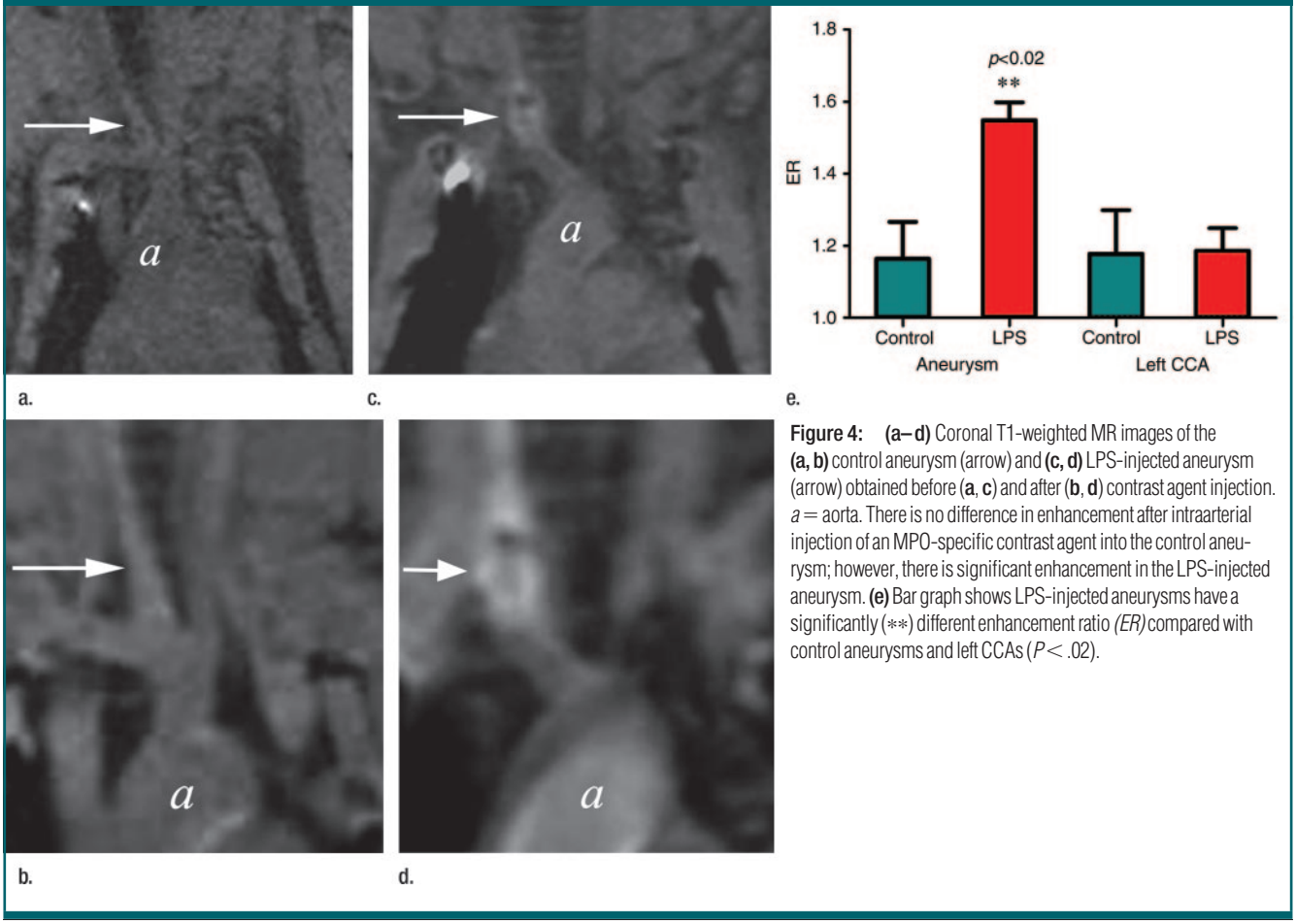

Figure 4: **(a–d)** Coronal T1-weighted MR images of the **(a, b)** control aneurysm (arrow) and **(c, d)** LPS-injected aneurysm (arrow) obtained before (**a**, **c**) and after (**b**, **d**) contrast agent injection. *a* = aorta. There is no difference in enhancement after intraarterial injection of an MPO-specific contrast agent into the control aneurysm; however, there is significant enhancement in the LPS-injected aneurysm. **(e)** Bar graph shows LPS-injected aneurysms have a significantly (**) different enhancement ratio *(ER)* compared with control aneurysms and left CCAs ($P < .02$).

pentetate dimeglumine prior to its injection into animals and observed corresponding increases in relaxivity in the presence of MPO and hydrogen peroxide. Use of di-5-hydroxytryptamide of gadopentetate dimeglumine has resulted in strong MR enhancement in basement membrane matrix gel implants and inflamed tissues in mice (28). Furthermore, use of the same contrast agent in rabbits has led to the visualization of MPO in atherosclerotic plaques (30).

While transgenic mice ($MPO^{-/-}$) have been used to reveal the specificity of di-5-hydroxytryptamide of gadopentetate dimeglumine for MPO in a model of myocardial ischemia and infarction (29), MPO-deficient rabbits are not available. Our results showed that di-5-hydroxytryptamide of gadopentetate dimeglumine is specific for MPO in our rabbit elastase model of aneurysm inflammation. We compared the observed enhancement ratio with that of di-tyrosine of gadopentetate dimeglumine, which is a contrast agent that is structurally similar to di-5-hydroxytryptamide of gadopentetate dimeglumine and has been demonstrated in vitro to be activated by peroxidases but not by MPO (24). Thus, it is unlikely that the site-specific T1-shortening effect seen in this study was caused by the nonspecific uptake of the contrast agent by inflammatory cells, since this is not the case in this or other animal models.

Our study had certain limitations. Procedural catheter manipulation and advancement of the modified tube through the aneurysm wall could have caused an intramural inflammatory response; this will be characterized in future studies. Furthermore, a fixed single concentration of LPS was used to induce inflammation. The amount and concentration of LPS could have influenced the magnitude and time course of inflammation induction. While inflammation is associated with IA progression and rupture in humans, the molecular environment in the aneurysm wall in the months, days, and hours prior to rupture is unknown (11,12,14). Only recently have the results of studies of IA pathogenesis in rats shown that inflammation plays a central role in IA progression (10,31). Macrophage infiltration and extracellular matrix degradation likely lead to defects in the vessel wall at the site of endothelial damage secondary to hemodynamic stress (10).

While it has been shown that the number of chronic intramural inflammatory changes are substantially increased in unruptured IAs compared with that in normal cerebral vessels (32), Frosen et al (14) went a step further to implicate acute intramural inflammatory cell infiltrates in ruptured IAs versus unruptured IAs. The results of a more recent study showed that nuclear factor-κ B, a family of transcription factors that regulates gene transcription in response to inflammatory mediators, is a key regulator of IA formation (31). Because of these findings, we chose to image MPO-mediated acute inflammation in experimentally-induced aneurysms rather than analyze a longer more chronic condition. As an area of future study, MPO imaging in aneurysms can be performed over a longer period of time after induction of inflammation with correlative in vitro MPO studies. Alternatively, a method with which to induce chronic inflammation can be assessed with MPO imaging. A previous study in which the authors used di-5-hydroxytryptamide of gadopentetate dimeglumine to image myocardial infarction showed that peak enhancement after left coronary artery ligation occurred 2 days after ligation and was 6.1 times higher at this time point than on day 8 (29).

To our knowledge, no studies have been performed to analyze MPO activity in ruptured versus unruptured aneurysms. To address this deficiency in the literature and further investigate the role of inflammation in aneurysm rupture, in our future research, we will examine resected human aneurysm tissue after microsurgical clip placement for MPO activity, with the goal being to correlate our animal model with clinical data.

The elastase model of aneurysm creation in the New Zealand white rabbit is well characterized and used for a variety of investigational purposes, including flow dynamics (33) and medical device testing (34). Aneurysms created with this method are similar to human IAs in size (35), wall thickness, and disruption of the internal elastic lamina (36). However, they are relatively devoid of intramural inflammation (36), providing the rationale for experimental inflammation induction. Other animal models of IA models exist, such as the rat model of renal hypertension and unilateral CCA ligation (37). However, IAs in these rats take anywhere from 1–3 months to form, the stage of IA formation varies widely among parallel animals, and IA formation rates may be as low as 10% (10). Inflammatory changes are present in these IAs (10,13) but are inconsistent. The rabbit model of aneurysm inflammation described in this article is technically feasible with successful induction of acute intramural inflammation with LPS. Endovascular delivery of proinflammatory agents, such as LPS, can be achieved with fluoroscopic guidance. Histologic and MPO-activity analyses enabled us to confirm that MPO was not present in the left CCA in the LPS-injected animals; this structure is in close proximity to the aneurysm. This was why we compared enhancement of the left CCA with that of the aneurysm at MR image analysis. Variability in MPO activity is accounted for by variable distribution of LPS in and around the aneurysm wall and variability in the host immune response to LPS. We believe that these principles combine with the predictable size and location (38) of elastase-induced aneurysms to serve as a reliable model with which to study aneurysm inflammation.

Practical applications: The use of MR contrast agents in molecular imaging has the potential to enhance our ability to diagnose a broad spectrum of diseases. As we advance our understanding of the pathogenesis of IA formation and progression, a noninvasive diagnostic test with which to depict active inflammation in aneurysms could serve as a valuable tool with which to identify patients at risk of IA rupture.

Acknowledgments: We are grateful to Philips Healthcare and Paul Dasari, BS, for his help with MR imaging.

References

1. Schievink WI. Intracranial aneurysms. N Engl J Med 1997;336:28–40.
2. Rosamond W, Flegal K, Furie K, et al. Heart

disease and stroke statistics: 2008 update—a report from the American Heart Association Statistics Committee and Stroke Statistics Subcommittee. Circulation 2008;117:e25–e146.

3. Johnston SC, Selvin S, Gress DR. The burden, trends, and demographics of mortality from subarachnoid hemorrhage. Neurology 1998;50:1413–1418.

4. International Study of Unruptured Intracranial Aneurysms Investigators. Unruptured intracranial aneurysms: risk of rupture and risks of surgical intervention. N Engl J Med 1998;339:1725–1733.

5. Wiebers DO, Whisnant JP, Huston J 3rd, et al. Unruptured intracranial aneurysms: natural history, clinical outcome, and risks of surgical and endovascular treatment. Lancet 2003;362:103–110.

6. Raymond J, Meder JF, Molyneux AJ, et al. Unruptured intracranial aneurysms: the unreliability of clinical judgment, the necessity for evidence, and reasons to participate in a randomized trial. J Neuroradiol 2006;33:211–219.

7. Vernooij MW, Ikram MA, Tanghe HL, et al. Incidental findings on brain MRI in the general population. N Engl J Med 2007;357:1821–1828.

8. Gonzalez CF, Cho YI, Ortega HV, Moret J. Intracranial aneurysms: flow analysis of their origin and progression. AJNR Am J Neuroradiol 1992;13:181–188.

9. Peters DG, Kassam AB, Feingold E, et al. Molecular anatomy of an intracranial aneurysm: coordinated expression of genes involved in wound healing and tissue remodeling. Stroke 2001;32:1036–1042.

10. Jamous MA, Nagahiro S, Kitazato KT, et al. Endothelial injury and inflammatory response induced by hemodynamic changes preceding intracranial aneurysm formation: experimental study in rats. J Neurosurg 2007;107:405–411.

11. Kataoka K, Taneda M, Asai T, Kinoshita A, Ito M, Kuroda R. Structural fragility and inflammatory response of ruptured cerebral aneurysms: a comparative study between ruptured and unruptured cerebral aneurysms. Stroke 1999;30:1396–1401.

12. Hashimoto T, Meng H, Young WL. Intracranial aneurysms: links among inflammation, hemodynamics and vascular remodeling. Neurol Res 2006;28:372–380.

13. Aoki T, Kataoka H, Morimoto M, Nozaki K, Hashimoto N. Macrophage-derived matrix metalloproteinase-2 and -9 promote the progression of cerebral aneurysms in rats. Stroke 2007;38:162–169.

14. Frosen J, Piippo A, Paetau A, et al. Remodeling of saccular cerebral artery aneurysm wall is associated with rupture: histological analysis of 24 unruptured and 42 ruptured cases. Stroke 2004;35:2287–2293.

15. Klebanoff SJ. Myeloperoxidase. Proc Assoc Am Physicians 1999;111:383–389.

16. Heinecke JW. Pathways for oxidation of low density lipoprotein by myeloperoxidase: tyrosyl radical, reactive aldehydes, hypochlorous acid and molecular chlorine. Biofactors 1997;6:145–155.

17. Fu X, Kassim SY, Parks WC, Heinecke JW. Hypochlorous acid oxygenates the cysteine switch domain of pro-matrilysin (MMP-7): a mechanism for matrix metalloproteinase activation and atherosclerotic plaque rupture by myeloperoxidase. J Biol Chem 2001;276:41279–41287.

18. Shabani F, McNeil J, Tippett L. The oxidative inactivation of tissue inhibitor of metalloproteinase-1 (TIMP-1) by hypochlorous acid (HOCI) is suppressed by anti-rheumatic drugs. Free Radic Res 1998;28:115–123.

19. Klebanoff SJ. Myeloperoxidase: friend and foe. J Leukoc Biol 2005;77:598–625.

20. Cawley CM, Dawson RC, Shengelaia G, Bonner G, Barrow DL, Colohan AR. Arterial saccular aneurysm model in the rabbit. AJNR Am J Neuroradiol 1996;17:1761–1766.

21. Cloft HJ, Altes TA, Marx WF, et al. Endovascular creation of an in vivo bifurcation aneurysm model in rabbits. Radiology 1999;213:223–228.

22. Engelmann MG, Redl CV, Nikol S. Recurrent perivascular inflammation induced by lipopolysaccharide (endotoxin) results in the formation of atheromatous lesions in vivo. Lab Invest 2004;84:425–432.

23. Philip D. Synthesis and spectroscopic characterization of gold nanoparticles. Spectrochim Acta A Mol Biomol Spectrosc 2008;71:80–85.

24. Querol M, Chen JW, Weissleder R, Bogdanov A Jr. DTPA-bisamide-based MR sensor agents for peroxidase imaging. Org Lett 2005;7:1719–1722.

25. Querol M, Chen JW, Bogdanov AA Jr. A paramagnetic contrast agent with myeloperoxidase-sensing properties. Org Biomol Chem 2006;4:1887–1895.

26. Niendorf HP, Haustein J, Cornelius I, Alhassan A, Clauss W. Safety of gadolinium-DTPA: extended clinical experience. Magn Reson Med 1991;22:222–228.

27. Chen JW, Pham W, Weissleder R, Bogdanov A Jr. Human myeloperoxidase: a potential target for molecular MR imaging in atherosclerosis. Magn Reson Med 2004;52:1021–1028.

28. Chen JW, Querol Sans M, Bogdanov A Jr, Weissleder R. Imaging of myeloperoxidase in mice by using novel amplifiable paramagnetic substrates. Radiology 2006;240:473–481.

29. Nahrendorf M, Sosnovik D, Chen JW, et al. Activatable magnetic resonance imaging agent reports myeloperoxidase activity in healing infarcts and noninvasively detects the antiinflammatory effects of atorvastatin on ischemia-reperfusion injury. Circulation 2008;117:1153–1160.

30. Ronald J, Chen JW, Rogers K, Querol M, Bogdanov A, Rutt B, Weissleder R. Molecular imaging of myeloperoxidase activity in rabbit atherosclerotic plaques. In: Proceedings of the 5th Annual Meeting of the Society for Molecular Imaging, Waikoloa, Hawaii, August 30 to September 2, 2006.

31. Aoki T, Kataoka H, Shimamura M, et al. NF-kappaB is a key mediator of cerebral aneurysm formation. Circulation 2007;116:2830–2840.

32. Chyatte D, Bruno G, Desai S, Todor DR. Inflammation and intracranial aneurysms. Neurosurgery 1999;45:1137–1146.

33. Seong J, Wakhloo AK, Lieber BB. In vitro evaluation of flow divertors in an elastase-induced saccular aneurysm model in rabbit. J Biomech Eng 2007;129:863–872.

34. Ding YH, Dai D, Lewis DA, Cloft HJ, Kallmes DF. Angiographic and histologic analysis of experimental aneurysms embolized with platinum coils, Matrix, and HydroCoil. AJNR Am J Neuroradiol 2005;26:1757–1763.

35. Short JG, Fujiwara NH, Marx WF, Helm GA, Cloft HJ, Kallmes DF. Elastase-induced saccular aneurysms in rabbits: comparison of geometric features with those of human aneurysms. AJNR Am J Neuroradiol 2001;22:1833–1837.

36. Abruzzo T, Shengelaia GG, Dawson RC 3rd, Owens DS, Cawley CM, Gravanis MB. Histologic and morphologic comparison of experimental aneurysms with human intracranial aneurysms. AJNR Am J Neuroradiol 1998;19:1309–1314.

37. Nagata I, Handa H, Hashimoto N, Hazama F. Experimentally induced cerebral aneurysms in rats. VI. Hypertension. Surg Neurol 1980;14:477–479.

38. Ding YH, Dai D, Lewis DA, et al. Can neck size in elastase-induced aneurysms be controlled? a prospective study. AJNR Am J Neuroradiol 2005;26:2364–2367.

Radiology 2009

This is your reprint order form or pro forma invoice

(Please keep a copy of this document for your records.)

Reprint order forms and purchase orders or prepayments must be received 72 hours after receipt of form either by mail or by fax at 410-820-9765. It is the policy of Cadmus Reprints to issue one invoice per order. **Please print clearly**.

Author Name _____
Title of Article _____
Issue of Journal_____ Reprint # _____ Publication Date _____
Number of Pages_____ KB # _____ Symbol Radiology
Color in Article? Yes / No (Please Circle)

Please include the journal name and reprint number or manuscript number on your purchase order or other correspondence.

Order and Shipping Information

Reprint Costs **(Please see page 2 of 2 for reprint costs/fees.)**

_____ Number of reprints ordered $_____
_____ Number of color reprints ordered $_____
_____ Number of covers ordered $_____
Subtotal $_____
Taxes $_____

(*Add appropriate sales tax for Virginia, Maryland, Pennsylvania, and the District of Columbia or Canadian GST to the reprints if your order is to be shipped to these locations*.)

First address included, add $32 for each additional shipping address $_____

TOTAL $_____

Shipping Address **(cannot ship to a P.O. Box) Please Print Clearly**

Name _____
Institution _____
Street _____
City _____ State _____ Zip _____
Country _____
Quantity_____ Fax _____
Phone: Day _____ Evening _____
E-mail Address _____

Additional Shipping Address* **(cannot ship to a P.O. Box)**

Name _____
Institution _____
Street _____
City _____ State _____ Zip _____
Country _____
Quantity _____ Fax _____
Phone: Day _____ Evening _____
E-mail Address _____

** Add $32 for each additional shipping address*

Payment and Credit Card Details

Enclosed: Personal Check _____
Credit Card Payment Details _____

Checks must be paid in U.S. dollars and drawn on a U.S. Bank.

Credit Card: __ VISA __ Am. Exp. __ MasterCard
Card Number _____
Expiration Date_____
Signature: _____

Please send your order form and prepayment made payable to:

Cadmus Reprints
P.O. Box 751903
Charlotte, NC 28275-1903

Note: Do not send express packages to this location, PO Box.

FEIN #:541274108

Invoice or Credit Card Information

Invoice Address **Please Print Clearly**

Please complete Invoice address as it appears on credit card statement

Name _____
Institution _____
Department _____
Street _____
City _____ State _____ Zip _____
Country _____
Phone _____ Fax _____
E-mail Address _____

Cadmus will process credit cards and *Cadmus Journal Services* will appear on the credit card statement.

If you don't mail your order form, you may fax it to 410-820-9765 with your credit card information.

Signature _____ Date _____

Signature is required. By signing this form, the author agrees to accept the responsibility for the payment of reprints and/or all charges described in this document.

RB-1/01/09

Radiology 2009

Black and White Reprint Prices

Domestic (USA only)						
# of Pages	50	100	200	300	400	500
1-4	$239	$260	$285	$303	$323	$340
5-8	$379	$420	$455	$491	$534	$572
9-12	$507	$560	$651	$684	$748	$814
13-16	$627	$698	$784	$868	$954	$1,038
17-20	$755	$845	$947	$1,064	$1,166	$1,272
21-24	$878	$985	$1,115	$1,250	$1,377	$1,518
25-28	$1,003	$1,136	$1,294	$1,446	$1,607	$1,757
29-32	$1,128	$1,281	$1,459	$1,632	$1,819	$2,002
Covers	$149	$164	$219	$275	$335	$393

International (includes Canada and Mexico)						
# of Pages	50	100	200	300	400	500
1-4	$299	$314	$367	$429	$484	$546
5-8	$470	$502	$616	$722	$838	$949
9-12	$637	$687	$852	$1,031	$1,190	$1,369
13-16	$794	$861	$1,088	$1,313	$1,540	$1,765
17-20	$963	$1,051	$1,324	$1,619	$1,892	$2,168
21-24	$1,114	$1,222	$1,560	$1,906	$2,244	$2,588
25-28	$1,287	$1,412	$1,801	$2,198	$2,607	$2,998
29-32	$1,441	$1,586	$2,045	$2,499	$2,959	$3,418
Covers	$211	$224	$324	$444	$558	$672

Color Reprint Prices

Domestic (USA only)						
# of Pages	50	100	200	300	400	500
1-4	$247	$267	$385	$515	$650	$780
5-8	$297	$435	$655	$923	$1194	$1467
9-12	$445	$563	$926	$1,339	$1,748	$2,162
13-16	$587	$710	$1,201	$1,748	$2,297	$2,843
17-20	$738	$858	$1,474	$2,167	$2,846	$3,532
21-24	$888	$1,005	$1,750	$2,575	$3,400	$4,230
25-28	$1,035	$1,164	$2,034	$2,986	$3,957	$4,912
29-32	$1,186	$1,311	$2,302	$3,402	$4,509	$5,612
Covers	$149	$164	$219	$275	$335	$393

International (includes Canada and Mexico))						
# of Pages	50	100	200	300	400	500
1-4	$306	$321	$467	$642	$811	$986
5-8	$387	$517	$816	$1,154	$1,498	$1,844
9-12	$574	$689	$1,157	$1,686	$2,190	$2,717
13-16	$754	$874	$1,506	$2,193	$2,883	$3,570
17-20	$710	$1,063	$1,852	$2,722	$3,572	$4,428
21-24	$1,124	$1,242	$2,195	$3,231	$4,267	$5,300
25-28	$1,320	$1,440	$2,541	$3,738	$4,957	$6,153
29-32	$1,498	$1,616	$2,888	$4,269	$5,649	$7028
Covers	$211	$224	$324	$444	$558	$672

Minimum order is 50 copies. For orders larger than 500 copies, please consult Cadmus Reprints at 800-407-9190.

Reprint Cover

Cover prices are listed above. The cover will include the publication title, article title, and author name in black.

Shipping

Shipping costs are included in the reprint prices. Domestic orders are shipped via FedEx Ground service. Foreign orders are shipped via a proof of delivery air service.

Multiple Shipments

Orders can be shipped to more than one location. Please be aware that it will cost $32 for each additional location.

Delivery

Your order will be shipped within 2 weeks of the journal print date. Allow extra time for delivery.

Tax Due

Residents of Virginia, Maryland, Pennsylvania, and the District of Columbia are required to add the appropriate sales tax to each reprint order. For orders shipped to Canada, please add 7% Canadian GST unless exemption is claimed.

Ordering

Reprint order forms and purchase order or prepayment is required to process your order. Please reference journal name and reprint number or manuscript number on any correspondence. You may use the reverse side of this form as a proforma invoice. Please return your order form and prepayment to:

Cadmus Reprints
P.O. Box 751903
Charlotte, NC 28275-1903

Note: Do not send express packages to this location, PO Box.
FEIN #:541274108

Please direct all inquiries to:

Rose A. Baynard
800-407-9190 (toll free number)
410-819-3966 (direct number)
410-820-9765 (FAX number)
baynardr@cadmus.com (e-mail)

Reprint Order Forms and purchase order or prepayments must be received 72 hours after receipt of form.